

Final Technical Report

Analysis of Southern California Seismicity Using Improved Locations, Focal Mechanisms and Stress Drops

Award G15AP00094

Peter M. Shearer
Institute of Geophysics and Planetary Physics
Scripps Institution of Oceanography
University of California, San Diego
La Jolla, CA 92093
858-534-2260 (phone), 858-534-5332 (fax)
pshearer@ucsd.edu

Term: 1 July 2015 to 30 June 2016

Research supported by the U.S. Geological Survey (USGS), Department of the Interior, under USGS award number G15AP00094. The views and conclusions contained in this document are those of the authors and should not be interpreted as necessarily representing the official policies, either expressed or implied, of the U.S. Government.

Award G15AP00094

ABSTRACT

We are analyzing earthquakes recorded by seismic networks in southern California to build on recent improvements in earthquake locations and source characterization. Our work focuses on systematically estimating earthquake source properties, such as stress drop and radiated energy, using P-wave spectra, and on modeling the scattering and attenuation structure of the southern California crust using coda waves. Building on the catalog of over 60,000 stress drop estimates that we published over a decade ago, our P-wave spectra analyses include a detailed comparison with other methods, such as the traditional empirical (EGF) approach of Abercrombie (1995), and improved uncertainty estimates that take into account the limited data bandwidth. We are using these results to test issues of earthquake scaling and our previous discovery that swarms and foreshock sequences in southern California tend to have lower-than-average stress drops. In addition, we are characterizing and modeling the P- and S-wave coda (scattering envelope) of earthquakes in southern California to resolve the scattering and attenuation structure of the crust using a Monte Carlo seismic phonon modeling method based on radiative transfer theory. In the long run, our results will provide basic knowledge about earthquake behavior and crustal properties that will increase the ability of seismologists to make realistic forecasts regarding strong motion probabilities in different locations, thus contributing to the goal of reducing losses from earthquakes in the United States.

Results

Earthquake source properties from P-wave spectra

Small earthquakes form the overwhelming majority of local earthquake records, but only their locations and magnitudes are routinely cataloged. To understand earthquake physics, scaling relations, and the evolving stress state within southern California, we need to go beyond this. Earthquake stress drop, proportional to the slip divided by the length scale of rupture, is a basic property of earthquakes and is fundamental to the physics of the source and its energy budget (e.g. Kanamori and Brodsky, 2004). Knowledge of the true variability of stress drop is also important for strong ground motion modeling and prediction (e.g., Cotton et al., 2013). Stress drop is commonly estimated by measuring the corner frequency of the seismic source spectrum and assuming a simplified theoretical model of rupture (e.g. Brune, 1970; Madariaga, 1976; Kaneko and Shearer, 2014, 2015). The large number of stress drop studies attest to their importance, but their widely varying results (~0.1 to 100 MPa), the large uncertainties (when calculated), and the ongoing controversy of whether stress drop changes with earthquake magnitude are evidence for how hard it is to calculate reliably (e.g., Abercrombie, 2013; Abercrombie and Rice, 2005; Shearer et al., 2006; Malagnini et al., 2013; Kwiatek et al., 2011, and references therein). This uncertainty limits the use stress drop studies in understanding spatial variations in stress state (e.g., Hauksson, 2014), and predicting strong ground motion (e.g., Baltay et al., 2013).

The main problem in calculating earthquake stress drop is how to separate source and path effects in band-limited signals and so measure corner frequency reliably. The problem becomes most acute for earthquakes where the corner frequency is outside the signal bandwidth. Various forms of empirical Green's function (EGF) analysis, in which the seismogram of a co-located small earthquake is used to represent the path effects in a larger earthquake recording, should decrease the trade-offs inherent in extracting the source spectrum (e.g., Kwiatek et al., 2014). If multiple earthquakes, recorded at multiple stations, are combined then it is possible to invert for both source parameters (constant for each event) and path effects (constant for individual paths) (e.g., Shearer et al., 2006; Oth et al., 2011).

Using the latter approach, in 2006 we analyzed over 60,000 earthquakes in southern California. Applying an iterative stacking approach to P-wave spectra, we were able to isolate source-, receiver-, and path-dependent terms. Estimated Brune-type stress drops ranged from 0.2 to 20 MPa with no dependence on moment. Despite the large scatter in observed stress drop, spatially coherent variations in median stress drop were apparent, including low values for the Imperial Valley and Northridge aftershocks and higher values for the eastern Transverse ranges. These results are intriguing and still represent the largest stress-drop study ever performed. However, the study suffered from the following limitations:

- (1) We analyzed data only between 1989 and 2001, a relatively stable period for the SCSN network, but which excluded more recent upgrades to broadband stations and the many additional earthquakes occurring in the last 15 years.

(2) Although our approach applies a version of the EGF correction, it does so by simultaneously fitting a large number of stacked source spectra to a single self-similar source model. While this has the advantage that small earthquakes can be retained in the analysis (i.e., they are not simply calibration events for study of larger events), it has the disadvantage of potentially biasing the results toward self-similarity (i.e., no scaling of stress drop with moment).

(3) The 20 Hz upper bandwidth limit is generally below the corner frequencies of the small events (by far the most numerous in the data set), meaning that their corner frequency estimates are highly uncertain because they rely on the extrapolation of small spectral differences.

(4) Comparisons to stress drop estimates obtained with more traditional EGF methods show only a very weak correlation, calling into question their reliability.

(5) No error bars or formal uncertainties are included with the stress drop estimates.

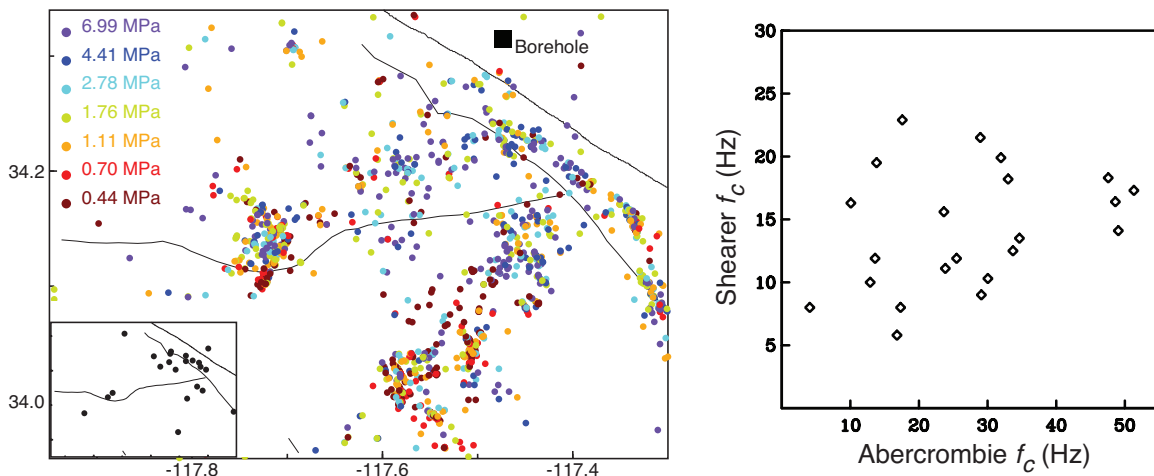


Figure 1. (left) Stress drop estimates for 1536 earthquakes near the junction of the San Andreas and San Jacinto faults computed by Shearer et al. (2006). 33 of these events were also analyzed by Abercrombie (1995), as shown in the inset. (right) A comparison of corner frequency estimates between the two studies, for those events recorded by 10 or more surface stations.

The last two problems are illustrated in Figure 1, which plots results from a comparison for 33 earthquakes in the Shearer et al. (2006) catalog that were also studied using the deep borehole recordings at Cajon Pass by Abercrombie (1995) and Abercrombie and Rice (2005). There is a weak correlation in the corner frequency estimates but with a huge amount of scatter. This is not unexpected, given that the Shearer et al. analysis is limited by the bandwidth of surface recordings and the Abercrombie study is based on only a single station and may be biased by azimuthal variations and the lack of suitable EGF events. But with such large scatter and without any uncertainty estimates, it is hard to know how much confidence to assign to any individual stress drop estimate.

We are now working to improve upon the Shearer et al. (2006) method in a number of respects. For example, we discovered that most events have good enough signal-to-noise

at high frequencies that the upper bandwidth limit can be extended to 30 Hz, which greatly improves corner frequency estimates for smaller earthquakes. We now also use the multitaper algorithm (e.g., Prieto et al., 2009), which provides smoother and more accurate spectra than the Hanning taper used in the 2006 study. In addition, we have improved the EGF fitting method and now apply an automatic algorithm to detect and discard clipped waveforms that can bias the spectral estimates.

But perhaps our most important improvement is in estimating errors and uncertainties. To address this, we have developed a set of error estimation techniques specific to source parameter estimates, based on nonparametric resampling theory (e.g., Efron and Tibshirani, 1994). These methods allow for robust error estimates in situations with complex relationships between the parameter of interest and the input data. Our method provides error estimates at each stage of the inversion procedure through random resampling of both the set of events and the set of stations over which iterative stacking is performed. Our results so far suggest that the dominant source of uncertainty comes from the varying spectra from different stations recording the same event, especially in cases where the event is observed by a small number of stations or has poor azimuthal station coverage. Another important result is that the uncertainty in corner frequency increases as the corner frequency approaches the signal bandwidth, which causes the confidence interval for each estimate to be asymmetric about the estimated value.

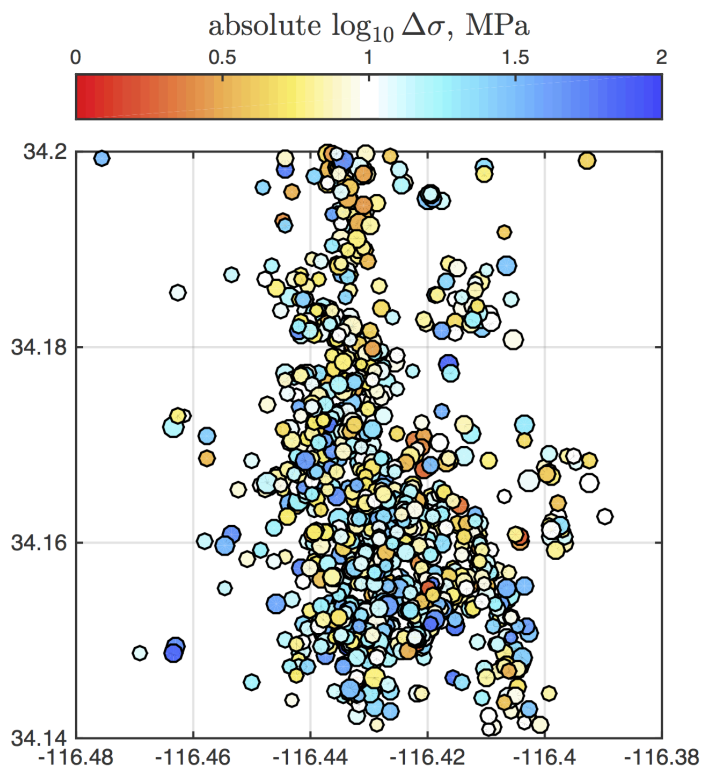


Figure 2. Map view of estimated stress drop D_s for earthquakes in the Landers region of southern California. Individual events are color-coded by stress drop (MPa, log-10 scale, with bluer colors meaning higher stress drop), and sized in proportion to magnitude.

Figure 2 shows preliminary results of the application of this improved methodology for the dense region of seismicity surrounding the epicenter of the 1992 Mw 7.3 Landers earthquake. Source spectral estimates are obtained for more than 1000 earthquakes from 1989–2001, most of them aftershocks of the Landers event. These events are a subset of

the total number of recorded events during this time period that meet strict quality control criteria designed to ensure reliability in the source parameter estimates. Corner frequencies, f_c , are estimated using the Brune (1970) model and stress drops are computed using the model of Madariaga (1976). Confidence intervals are computed for each corner frequency estimate using a combination of bootstrap and jackknife resampling of the event and station sets over which iterative stacking is performed. This error analysis is performed after a variance-stabilizing logarithmic transformation on f_c , and a student's T distribution is used following transformation to maintain accuracy in the confidence intervals for the events with smaller numbers of observations. Specific examples of the fits for two earthquakes are shown in Figure 3.

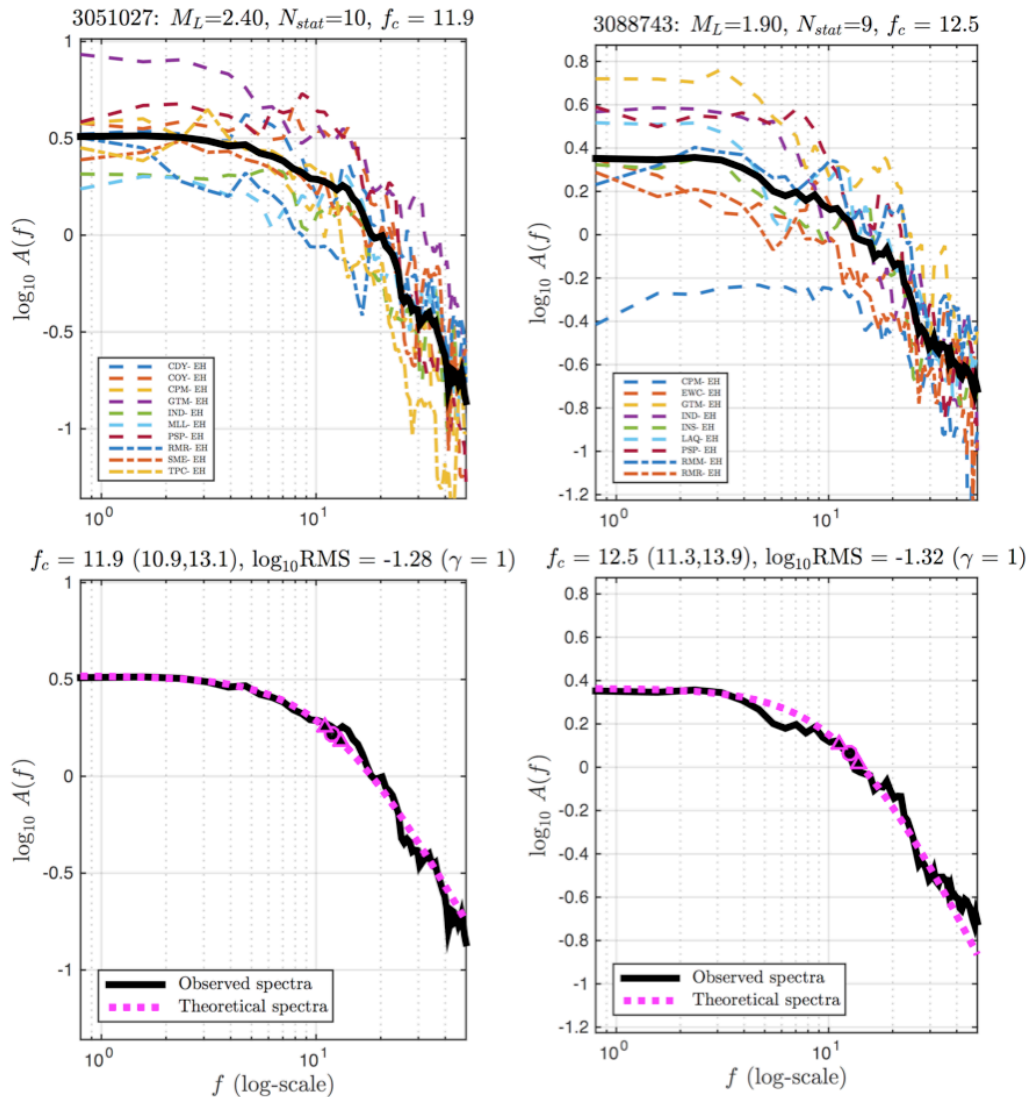


Figure 3. Example event spectra for two earthquakes in the Landers region with local magnitudes of 2.4 (left) and 1.9 (right). The top plots show single-station estimates of the each event spectra, while the bottom plots show the final estimate of the event spectra after stacking over all stations. Estimated corner frequencies (and 1-sigma confidence intervals) are listed at the top of each lower subplot, and used to generate the plots of theoretical spectra (pink, with corner frequency marked as a filled circle).

The stress drop estimates plotted in Figure 2 are correlated with previous results for this region from Shearer et al. (2006) but have greater spatial coherence and reduced scatter. There are systematically higher median stress drops in the south and southeast than in the north. Eventually we plan to compare these improved estimates with the mainshock slip distribution to see if higher stress drop aftershocks occur near the edges of large slip patches. We have also begun comparing these results with the traditional EGF methods of Abercrombie (1995) and others. The goal is to identify the strengths and limitations of each method. Toward this end, we have also begun comparing results for another test region of seismicity near Cajon Pass, where it is possible to incorporate data from a borehole seismometer. Ultimately, our goal is to produce an improved and greatly enlarged catalog of robust source parameter estimates for southern California from 1989 to 2015, which should prove invaluable in future studies of earthquake source physics, crustal stress, and seismic hazard.

Coda wave analyses

Body-wave arrivals seen in local and regional earthquake records are followed by a wavetrain of scattered energy termed the coda, which is typically modeled using scattering theories for random media. A number of classic studies have analyzed local earthquake coda, including Aki and Chouet (1975), Sato (1977), Wu (1985), Frankel and Wennerberg (1987), Fehler et al. (1992), and many others (see review by Sato and Fehler, 1998). Most of these studies have focused on understanding coda behavior in terms of models of crustal and upper-mantle scattering strength and intrinsic attenuation. However, it is also possible to use coda waves to examine the spectral properties of the earthquake source, i.e., to resolve source spectra and estimate stress drop and radiated energy (e.g., Mayeda and Walter, 1996; Baltay et al., 2011; Abercrombie, 2013). Coda-wave approaches to source spectral measurements have the great advantage that they tend to average out radiation pattern and directivity differences in the spectra observed at individual stations (see Kaneko and Shearer, 2014, 2015, for a recent account of the importance of these effects).

We have begun a comprehensive study of coda behavior in southern California to examine both crustal structure and source properties. This research is related to previous southern California work on attenuation structure (Hauksson and Shearer, 2006) and stress drop estimates from P-wave spectra (Shearer et al., 2006; Chen and Shearer, 2011; Goebel et al., 2015). Our approach has several stages: (1) stack coda envelopes from large numbers of earthquakes to obtain spatially averaged coda behavior as a function of distance, source depth, and frequency; (2) model these results using a multiple-scattering Monte Carlo seismic phonon algorithm (Shearer and Earle, 2004) to determine the best-fitting 1-D model of scattering properties and intrinsic attenuation; (3) compare these results to other methods, such as the multiple-lapse-time-window (MLTW) approach of Fehler et al. (1992); (4) analyze deviations of individual seismogram codas from the stacked average in order to characterize and model likely spatial variations in scattering strength; (5) apply methods similar to those developed by Mayeda and Walter (1996) and others to characterize source spectra for thousands of individual earthquakes.

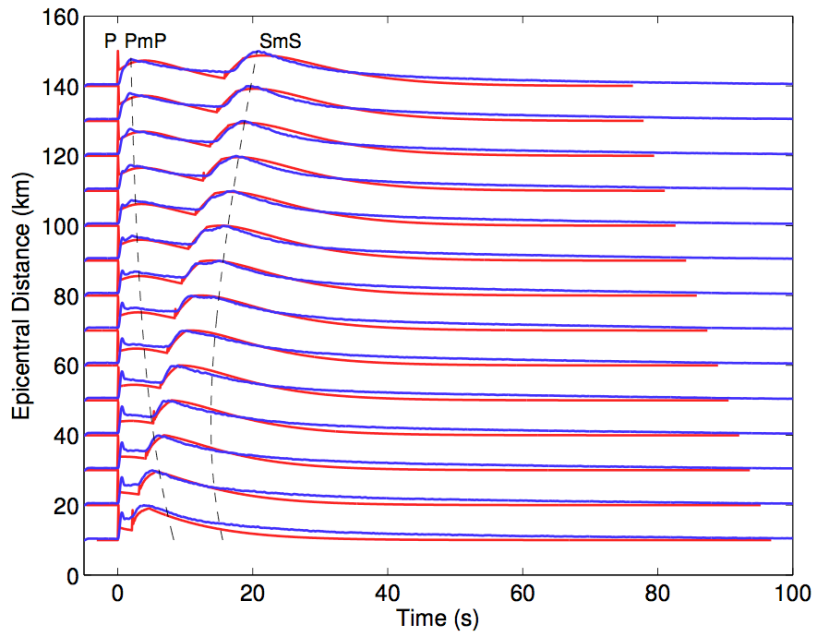


Figure 5. Blue lines show envelope-function stacks of 155,350 southern California seismograms, filtered from 2 to 4 Hz. Results are from 5306 earthquakes shallower than 5 km. Stacks are performed at 10 km intervals in epicentral distance. The red lines show the prediction of a simple analytical approximation to scattering in a whole space.

We have made substantial progress on many of these coda-related tasks. Figure 5 shows a preliminary stack of 155,350 coda wave envelopes at 2 to 4 Hz from 5306 earthquakes at source depths of 0 to 5 km. An empirical fit based on the whole-space approximate solution to the radiative transfer equations (Paasschens, 1997) as applied using the MLTW approach by Carcolé and Sato (2010) yields the red curve. This assumes intrinsic attenuation of $Q_p = 900$, $Q_s = 600$, mean free paths for both P and S waves of 17 km, and an S-to-P energy ratio of 12. Although the overall fit is reasonable, the model systematically underpredicts P coda at short distances and S coda at long times. In addition, the separation into Pn and PmP at long ranges is not described by the whole-space model.

More realistic coda models can be obtained by taking into account the free surface, velocity gradients in the crust, and the presence of the Moho. A versatile and powerful approach to simulating scattering in complex models is a computer-based Monte Carlo method to track the random trajectories of millions of seismic energy particles that are sprayed from the source and then subject to scattering probabilities derived from random media theories. Numerous authors have applied this approach (e.g., Gusev and Abubakirov, 1987; Hoshiya, 1991; Margerin et al., 2000) and we have written such a Monte Carlo code to simulate whole-Earth scattering (Shearer and Earle, 2004). The algorithm is fully elastic and includes both P- and S-wave single and multiple scattering. It computes scattering probabilities and scattering angles based on theoretical results for random heterogeneity models. The random medium is characterized by two parameters, the correlation distance, a , and the RMS fractional velocity fluctuation, e . We have adapted this code to work on local and regional scale scattering problems. The basic idea is illustrated in Figure 6.

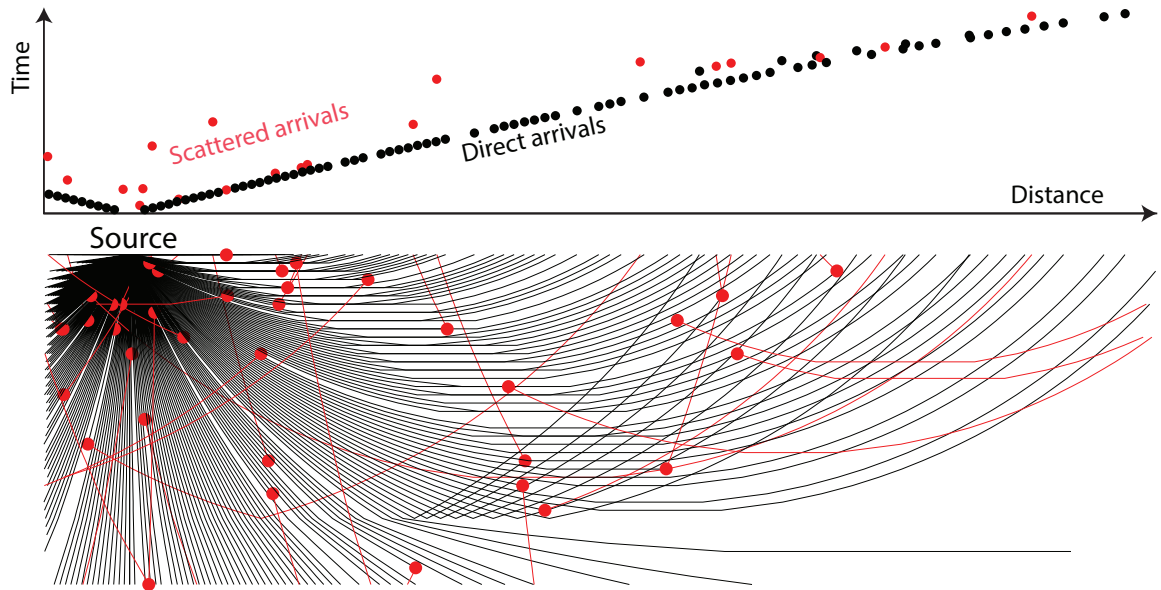


Figure 6. (bottom) Example ray paths for a Monte Carlo simulation of scattering. Rays are sprayed uniformly from a source and traced through a 1-D model. They are continuously subject to a scattering probability and tested for possible scattering events by using a random number generator. Direct (unscattered) waves are shown in black. Scattering events are shown as red circles, and the resulting perturbed ray paths are plotted in red. (top) Whenever a ray strikes the surface, the time and distance are saved in order to construct a time versus distance image of the energy in the wavefield.

Using this more realistic modeling algorithm, we have obtained good fits to both vertical and transverse-component coda stacks, as shown in Figure 7. We have found that the data require at least a two-layer model: a shallow crustal layer with strong wide-angle scattering and high intrinsic attenuation and a deeper layer with weaker scattering and lower intrinsic attenuation (top 5.5 km: $Q_p = 250$, $Q_s = 125$, $a = 50$ m, $e = 0.5$; lower crust; : $Q_p = 900$, $Q_s = 400$, $a = 2$ km, $e = 0.05$). Our calculation uses a realistic 1D velocity model for the southern California crust and includes surface and Moho reflections. The synthetic results generally fit quite well for both the P- and S- wave coda decay and the energy distribution between the direct and coda waves. However, there are a few discrepancies, such as a lack of modeled coda energy on the vertical component at short ranges and long lapse times. We are continuing to refine the model to try to understand where these differences may be coming from.

Figure 7 normalizes the amplitude of each range bin to the same value. It is important to also account for the amplitude decay with distance and we have achieved good overall fits to this with the model described above. A great advantage of our approach is that we are able to obtain unified, energy-conserving models that can explain all the main features that are seen in both direct waves and coda waves. The ultimate goal of this research is to understand, as a function of frequency, where the energy radiated from earthquakes is going, i.e., how much is contained in the direct wave arrivals, how much is scattered and where it goes, and how much is lost due to intrinsic attenuation. Although very interesting from the theoretical point of view in characterizing scattering properties and the power spectrum of crustal heterogeneity, this information is also fundamental for informing strong ground motion estimates at high frequencies, where scattering and

attenuation effects are critical. We plan to use these results to improve coda-based estimates of source spectral properties (e.g., Mayeda and Walter, 1996; Baltay et al., 2011; Abercrombie, 2013) and compare these results to those obtained from direct P-wave spectral analyses.

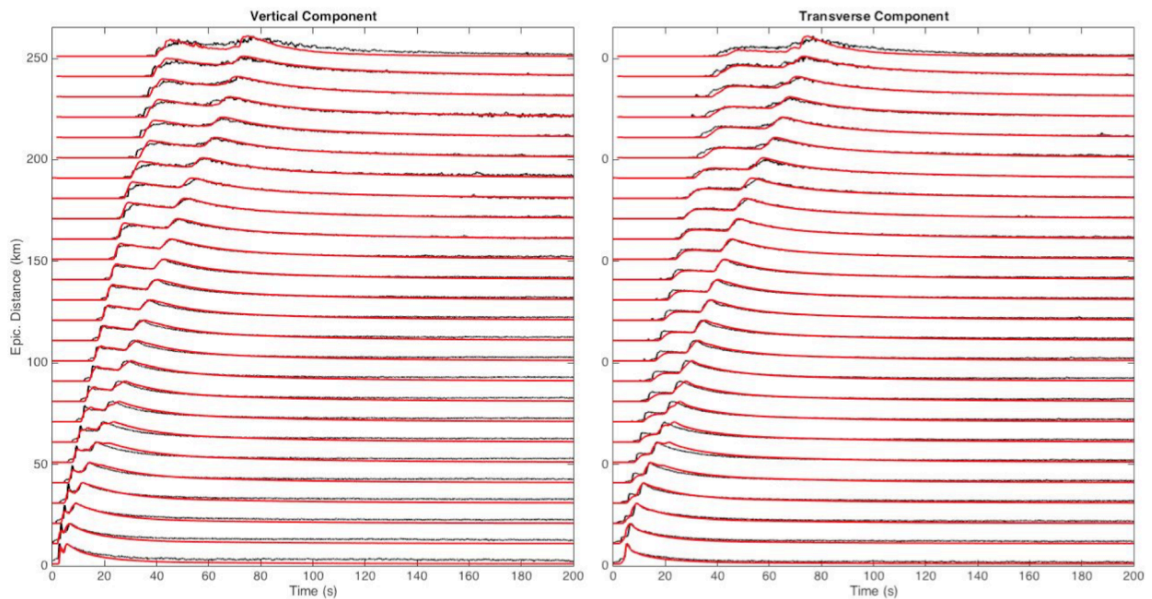


Figure 7. Black lines show envelope-function stacks of 31,895 vertical (left) and 29,191 transverse (right) southern California seismograms, filtered from 2 to 4 Hz. Results are from 9611 earthquakes at depths between 10 and 15 km. Stacks are performed at 10 km intervals in epicentral distance. The red lines show synthetic results from a Monte Carlo simulation based on 1D-layered southern California scattering model.

References

- Abercrombie, R. E., Earthquake scaling relationships from -1 to 5 ML using seismograms recorded at 2.5-km depth, *J. Geophys. Res.*, **100**, 24,915–24,936, 1995.
- Abercrombie, R. E., Comparison of direct and coda wave stress drop measurements for the Wells, Nevada, earthquake sequence, *J. Geophys. Res.*, **118**, 1458–1470, doi: 10.1029/2012JB009638, 2013.
- Abercrombie, R. E., and J. R. Rice, Small earthquake scaling revisited: can it constrain slip weakening? *Geophys. J. Int.*, **162**, 406–424, 2005.
- Aki, K., and B. Chouet, Origin of coda waves: source attenuation and scattering effects, *J. Geophys. Res.*, **80**, 3322–3342, 1975.
- Baltay, A. S., T. C. Hanks and G. C. Beroza, Stable stress drop measurements and their variability: implications for ground-motion prediction. *Bull. Seism. Soc. Am.*, **103**, doi: 10.1785/0120120161, 2013.
- Baltay, A., S. Ide, G. Prieto, and G. Beroza, Variability in earthquake stress drop and apparent stress, *Geophys. Res. Lett.*, doi: 10.1029/2011GL046698, 2011.
- Brune, J., Tectonic stress and the spectra of seismic shear waves from earthquakes, *J. Geophys. Res.*, **75**, 4997–5009, 1970.
- Carcolé, E., and H. Sato H., Spatial distribution of scattering loss and intrinsic absorption of short-period S waves in the lithosphere of Japan on the basis of the multiple lapse time

- window analysis of Hi-net data, *Geophys. J. Int.*, **180**, 268–290, doi: <http://dx.doi.org/10.1111/j.1365-246X.2009.04394.x>, 2010.
- Chen, X. and P. M. Shearer, Comprehensive analysis of earthquake source spectra and swarms in the Salton Trough, California, *J. Geophys. Res.*, **116**, doi: 10.1029/2011JB008263, 2011.
- Cotton, F., R. Archuleta and M. Causse, What is the sigma of the stress drop? *Seismol. Res. Letts.*, **84**, 42-48, doi: 10.1785/0220120087, 2013.
- Efron, B., and R. J. Tibshirani, *An Introduction to the Bootstrap*, CRC Press, Boca Raton, Florida, 1994.
- Fehler M., M. Hoshiya, H. Sato, and K. Obara, Separation of scattering and intrinsic attenuation for the Kanto-Tokai region, Japan, using measurements of S-wave energy versus hypocentral distance. *Geophys. J. Int.*, **198**, 787-800, 1992.
- Frankel, A., and L. Wennerberg, Energy-flux model of seismic coda: separation of scattering and intrinsic attenuation, *Bull. Seismol. Soc. Am.*, **77**, 1223-1251, 1987.
- Goebel, T. H. W., E. Hauksson, P. M. Shearer, and J. P. Ampuero, Stress drop heterogeneity within tectonically complex regions: A case study of San Geronio Pass, southern California, *Geophys. J. Int.*, **202**, 514–528, 2015.
- Gusev, A. A., and I. R. Abubakirov, Monte-Carlo simulation of record envelope of a near earthquake, *Phys. Earth Planet. Int.*, **49**, 30-36, 1987.
- Hauksson, E., Average Stress Drops of Southern California Earthquakes in the Context of Crustal Geophysics: Implications for Fault Zone Healing, *Pure Appl. Geophys.*, 1–12, doi:10.1007/s00024-014-0934-4, 2014.
- Hauksson, E., and P. M. Shearer, Attenuation models (Qp and Qs) in three dimensions of the southern California crust: Inferred fluid saturation at seismogenic depths, *J. Geophys. Res.*, **111**, B05302, doi:10.1029/2005JB003947, 2006.
- Hoshiya, M., Simulation of multiple-scattered coda wave excitation based on the energy conservation law, *Phys. Earth Planet. Int.*, **67**, 123-136, 1991.
- Kanamori, H. and E. E. Brodsky, The physics of earthquakes, *Reports on Progress in Physics*, **67**, 1429 - 1496, DOI:10.1088/0034-4885/67/8/R03, 2004.
- Kaneko, Y., and P. M. Shearer, Seismic source spectra and estimated stress drop from cohesive-zone models of circular subshear rupture, *Geophys. J. Int.*, doi: 10.1093/gji/ggu030, 2014.
- Kaneko, Y., and P. M. Shearer, Variability of seismic source spectra, estimated stress drop and radiated energy, derived from cohesive-zone models of symmetrical and asymmetrical circular and elliptical ruptures, *J. Geophys. Res.*, **120**, doi: 10.1002/2014JB011642, 2015.
- Kwiatek, G., Bulut, F., Bohnhoff, M., Dresen, G., High-resolution analysis of seismicity induced at Berlín geothermal field, El Salvador, *Geothermics*, **52**, 98-111, doi: org/10.1016/j.geothermics.2013.09.008, 2014.
- Madariaga, R., Dynamics of an expanding circular fault, *Bull. Seism. Soc. Am.*, **66**, 639–666, 1976
- Malagnini, L., K. Mayeda, S. Nielsen, S.-H. Yoo, I. Munafo, C. Rawles, and E. Boschi, Scaling transition in earthquake sources: a possible link between seismic and laboratory measurements, *Pur. Appl. Geophys.*, **171**, doi: 10.1007/s00024-013-0749-8, 2013.
- Margerin, L., M. Campillo, and B. V. Tiggelen, Monte Carlo simulation of multiple scattering of elastic waves, *J. Geophys. Res.*, **105**, 7873-7892, 2000.
- Mayeda, K. and W.R. Walter, Moment, energy, stress drop, and source spectra of western United States earthquakes from regional coda envelopes, *J. Geophys. Res.*, **101**, 11,195-11,208, 1996.
- Oth, A., D. Bindi, S. Parolai and D. Di Giacomo, Spectral analysis of K-NET and KiK-net data in Japan, Part II: On attenuation characteristics, source spectra, and site response of borehole and surface stations. *Bull. Seismol. Soc. Am.*, **101**, 667-687, doi: 10.1785/0120100135, 2011.
- Paasschens, J. C. J., Solution of the time-dependent Boltzmann equation, *Phys. Rev. E*, **56**, 1135, doi: <http://dx.doi.org/10.1103/PhysRevE.56.1135>, 1997.

- Prieto, G., R. Parker, and F. Vernon, A Fortran 90 library for multitaper spectrum analysis, *Computers and Geosciences*, **35**, 1701–1710, doi: 10.1016/j.cageo.2008.06.007, 2009.
- Sato, H., Energy propagation including scattering effects, single isotropic scattering approximation. *J. Phys. Earth*, **25**, 27-41, 1977.
- Sato, H., and M.C. Fehler, *Seismic Wave Propagation and Scattering in the Heterogeneous Earth*, Springer-Verlag, New York, 1998.
- Shearer, P. M., G. A. Prieto, and E. Hauksson, Comprehensive analysis of earthquake source spectra in southern California, *J. Geophys. Res.*, **111**, B06303, doi:10.1029/2005JB003979, 2006.
- Shearer, P.M. and P.S Earle, The global short-period wavefield modelled with a Monte Carlo seismic phonon method, *Geophys. J. Int.*, **158**, 1103-1117, 2004.
- Wu, R.-S., Multiple scattering and energy transfer of seismic waves—separation of scattering effect from intrinsic attenuation—I. Theoretical modelling, *Geophys. J. Roy. Astron. Soc.*, **82**, 57-80, 1985.

Bibliography (Reports Published since 2011)

- Chen, X., and P. M. Shearer, Comprehensive analysis of earthquake source spectra and swarms in the Salton Trough, California, *J. Geophys. Res.*, **116**, B09309, doi:10.1029/2011JB008263, 2011.
- Chen, X., and P. M. Shearer, California foreshock sequences suggest aseismic triggering process, *Geophys. Res. Lett.*, **40**, doi:10.1002/grl.50444, 2013.
- Chen, X., and P. M. Shearer, Analysis of foreshock sequences in California and implications for earthquake triggering, *Pure Appl. Geophys.*, doi: 10.1007/s00024-015-1103-0, 2015.
- Chen, X., P. M. Shearer, and R. E. Abercrombie, Spatial migration of earthquakes within seismic clusters in Southern California: Evidence for fluid diffusion, *J. Geophys. Res.*, **117**, B04301, doi:10.1029/2011JB008973, 2012.
- Goebel, T. H. W., E. Hauksson, P. M. Shearer, and J. P. Ampuero, Stress drop heterogeneity within tectonically complex regions: A case study of San Geronio Pass, southern California, *Geophys. J. Int.*, **202**, 514–528, 2015.
- Hauksson, E., J Stock, R. Bilham, M. Boese, X. Chen, E. H. Fielding, J. Galetzka, K. W. Hudnut, K. Hutton, L. C. Jones, H. Kanamori, P. M. Shearer, J. Steidl, J. Treiman, S. Wei, and Wenzheng Yang, Report on the August 2012 Brawley earthquake swarm in Imperial Valley, Southern California, *Seismol. Res. Lett.*, **84**, 177-189, doi: 10.1785/0220120169, 2013.
- Kane, D. L., G. A. Prieto, F. L. Vernon, and P. M. Shearer, Quantifying seismic source parameter uncertainties, *Bull. Seismol. Soc. Am.*, **101**, 535–543, doi: 10.1785/0120100166, 2011.
- Kane, D. L., P. M. Shearer, B. P. Goertz-Allmann, and F. L. Vernon, Rupture directivity of small earthquakes at Parkfield, *J. Geophys. Res.*, **118**, doi: 10.1029/2012JB009675, 2013.
- Yang, Z., A. Sheehan, and P. Shearer, Stress-induced upper crustal anisotropy in southern California, *J. Geophys. Res.*, **116**, doi: 10.1029/2010JB007655, 2011.
- Shearer, P. M., Self-similar earthquake triggering, Båth's law, and foreshock/aftershock magnitudes: Simulations, theory, and results for southern California, *J. Geophys. Res.*, **117**, B06310, doi: 10.1029/2011JB008957, 2012.

- Shearer, P. M., Space-time clustering of seismicity in California and the distance dependence of earthquake triggering, *J. Geophys. Res.*, **117**, B10306, doi: 10.1029/2012JB009471, 2012.
- Shearer, P. M., Reply to comment by S. Hainzl on “Self-similar earthquake triggering, Båth’s Law, and foreshock/aftershock magnitudes: Simulations, theory and results for southern California,” *J. Geophys. Res.*, **118**, doi: 10.1002/jgrb.50133, 2013.
- Smith-Konter, B. R., D. T. Sandwell, and P. Shearer, Locking depths estimated from geodesy and seismology along the San Andreas Fault System: Implications for seismic moment release, *J. Geophys. Res.*, **116**, doi: 10.1029/2010JB008117, 2011.
- Sumiejski, P. E., and P. M. Shearer, Temporal stability of coda Q^{-1} in southern California, *Bull. Seismol. Soc. Am.*, **102**, 873–877, doi: 10.1785/0120110181, 2012.
- Trugman, D.T., P. M. Shearer, A. A. Borsa, and Y. Fialko, A comparison of long-term changes in seismicity at the Geysers, Salton Sea, and Coso geothermal fields, *J. Geophys. Res.*, **121**, doi: 10.1002/2015JB012510, 2016.
- Uchide, T., H. Yao, and P. M. Shearer, Spatio-temporal distribution of fault slip and high-frequency radiation of the 2010 El Mayor-Cucapah, Mexico earthquake, *J. Geophys. Res.*, **118**, doi: 10.1002/jgrb.50144, 2013.
- Zhang, Q., and P. M. Shearer, A new method to identify earthquake swarms applied to seismicity near the San Jacinto Fault, California, *Geophys. J. Int.*, **205**, doi: 10.1093/gji/ggw073, 2016.